Oscillating color transparency in $\pi A \to \pi p(A-1)$ and $\gamma A \to \pi N(A-1)$

Pankaj Jain
Department of Physics, IIT Kanpur, Kanpur 208 016, India

Bijoy Kundu
Physics Department, University of Virginia, Charlottesville, Virginia 22903

John P. Ralston
Department of Physics and Astronomy, University of Kansas, Lawrence, Kansas 66045

(Received 5 January 2001; revised manuscript received 22 February 2002; published 9 May 2002)

We study the energy dependence of 90° c.m. fixed angle scattering of $\pi p \to \pi' p'$ and $\gamma p \to \pi^+ n$ at large momentum transfer. The experimental data are found to be well described in terms of complex interfering short and long distance amplitudes with dynamical phases induced by Sudakov effects. We calculate the color transparency ratio for the corresponding processes in nuclear environments $\pi A \to \pi' p(A-1)$ and $\gamma A \to \pi N(A-1)$, taking nuclear filtering into account. We predict that the transparency ratio for these reactions will oscillate with energy. This provides an important test of the Sudakov phase shift and nuclear filtering hypothesis, which can be checked in upcoming experiments.

DOI: 10.1103/PhysRevD.65.094027 PACS number(s): 13.85.Dz, 14.20.Dh, 14.40.−n

I. INTRODUCTION

The strong interactions remain a mystery and a phenomenology. Color transparency separates conventional strong interaction physics from perturbative QCD. The perturbative calculation predicts *suppression* of strong interactions in certain exclusive reactions containing a large momentum transfer $Q^2 \gg \mathrm{GeV}^2$ subprocess [1,2]. Suppression is supposed to occur in initial or final state interactions with nuclear targets. The perturbative QCD (PQCD) prediction is dramatic because it apparently contradicts the older theory in a domain of its validity [1,2]. Indeed it is not clear whether color transparency is capable of being described using hadronic coordinates [3]. At the same time, the many shortcomings of the PQCD description at the moderate momentum transfer values of experiments [4,7] are well known: hence the phenomena of color transparency play a pivotal role from either point of view.

The BNL E850 experiment of Carroll *et al.* [4] compared proton-proton elastic collisions with corresponding quasi-elastic nuclear processes $pA \to p'p''(A-1)$. The transparency ratio showed a bump as a function of energy. The origin of the bump [8,9] has been controversial, and the underlying mechanism has often been assumed to be unique to proton-proton reactions. In Ref. [8] it was predicted that the transparency ratio oscillates 180° out of phase with the oscillations in free space pp elastic scattering. The bump observed in the transparency ratio is then interpreted as a segment of these oscillations. Higher energy experiments would be able to verify the prediction of oscillations. If confirmed this will also rule out the alternative hypothesis [9] which interprets the bump in terms of a charm threshold effect. Very recently, the BNL E850 group [5] has released results of improved and extended measurements, which confirm the original data and extend it slightly.

Here we show that *oscillatory color transparency* is also expected in several processes involving the pion. We report calculations predicting new phenomena observable in experiments currently underway at CEBAF [10], which may provide fundamental information on how PQCD may be applied to exclusive processes both in free space and in a nuclear medium. Other experimental predictions can be checked at BNL or other hadron beam laboratories. The predictions are rather distinctive, and tests of the entire framework of color transparency become available.

II. FRAMEWORK

Consider the reaction $\pi p \to m'N'$ compared to $\pi A \to m'N'(A-1)$, where m' represents a meson and N' represents a nucleon. The nuclear target serves both as a probe and as a modifier of the corresponding free-space process. Let t be the Mandlestam variable for momentum transfer squared by the mesons, s be the center of mass energy squared, and assume both s and $|t|$ are large compared to GeV^2. We will be concerned with the fixed angle limit $s/t = \mathrm{const}$, whereby the cross section $d\sigma/dt|_\theta$ is a function of s. In this limit it is argued that the participating quarks are at short distances relative to one another: the presence or absence of a nuclear target provides ways to test this experimentally.

Despite the popularity and immense impact of the quark-counting factorization scheme [11], and the common misconception that it defines the approach of PQCD, we must explain the reasons that this is not our framework. The meson scattering processes contain Landshoff pinch singularities [12,13] which are particularly relevant. In PQCD the pinch singularities allow hard scattering processes to proceed without obliging all constituents to be at a relatively short distance. Note that the *subsets* of constituents which actually collide have a short-distance interaction. Meanwhile the separation between different, independent collisions is not kinematically small. The pinch integration regions in PQCD are dominated by Sudakov effects [14,15] represented na-

ively by the exponentiation of $-a\log^2(s/\lambda_1^2)+i\pi b\log(s/\lambda_2^2)$, where λ_1^2,λ_2^2 are fixed scales and a,b are parameters. The exponentiation of $i\pi\log(s)$ terms associated with $\log^2(s-i\epsilon)$ terms is very general, and can be viewed as a necessary consequence of analyticity [16]. The existence of this complex phase structure has been shown to be a consistent prediction of factorization and perturbative QCD [16,17,15]. Interference of the energy-dependent phase is expected to reveal itself via oscillations in $d\sigma/dt|_\theta$ as a function of energy.

The physics of pinch singularities, and Sudakov effects, demands a factorization scheme more general than the asymptotic short-distance ''quark-counting'' method [11]. To represent all the diagrams and integration regions, we take this into account, and include integrations over the transverse spatial separation b between quarks [15,18]. We call this ''impact-parameter factorization.'' After the transverse integrations are done, one may take the *asymptotic* limit of $s\to\infty$, or study the limit of $s\gg\mathrm{GeV}^2$. These two limits are not the same: both are equally valid approaches to PQCD, and we wish to emphasize that the term ''asymptotic'' is not synonymous with ''large'' or ''perturbative.'' There is a third procedure, which is to take the asymptotic limit of *short distance* in the first step, producing the distribution amplitudes: this limit is distinct from the other two.

A. Factorization versus short distance

Some time ago, Mueller [19] showed that integration over the Sudakov factors reproduced power-law behavior in an asymptotic saddle-point approximation to $pp\to pp$ fixed-angle scattering. Botts and Sterman [15] confirmed this feature with impact-parameter factorization, pointing out the regulation of Sudakov effects via integrations over the transverse spatial separation b between quarks. The Sudakov effects strongly damp amplitudes with large $b\sim 1/\Lambda_{QCD}$, but are negligible at asymptotically short distances. The asymptotically dominant integration region is somewhat in between, yet approaches $b\to 0$ as $s\to\infty$. It is significant that the power law obtained is not that of quark counting. Moreover, the power is such that the independent scattering contributions remain the leading contributions as $s\to\infty$.

At the same time, the impact-parameter factorization predicts oscillations in the fixed-angle amplitude at finite s. The method employs the concept of a purely imaginary anomalous dimension, first suggested in Ref. [16] and later established in great detail [17]. The use of a transverse degree of freedom also retains the impulse approximation and concept of factorization between a calculable hard scattering and universal hadronic wave functions. However the factorization is more complicated than that of deeply inelastic scattering and the operator-product expansion.

In contrast, the quark-counting method [20] prescribes a method of taking $b\to 0$ in the first step. Universal ''distribution amplitudes'' can then be defined which are calculated purely on the basis of short-distance physics, and which do not depend on the process of measurement. An operator product expansion applies. If there are no pinches the quark-counting method may reproduce the asymptotic limit of impact-parameter factorization. In general, however, the integration regions differ, and the approximations differ, as shown by the different power behavior. There is no contradiction in generating two different asymptotic limits, because the quark-counting model neglects the independent scattering contributions, which contradict the assumption that hard scattering requires short distance.

Finally there is the case of $s\gg\mathrm{GeV}^2$ *but s not asymptotically large*. This concept is simple, but confused in the literature, perhaps because PQCD was earlier associated with ''asymptotic freedom.'' We maintain that s must be large enough for the perturbative approach to be self-consistent—we would prefer $s\gg\mathrm{GeV}^2$, but no PQCD analysis ever specifies an exact cutoff energy. We also maintain that terms such as ''$s\to\infty$'' are meaningless, or at least so conceptually dangerous as to be of little use, and we apply our work to $s\gg\mathrm{GeV}^2$ as a *conceptually separate perturbative regime* from the asymptotic one. A mathematical example may suffice: one of the earliest asymptotic approximations is Stirling's $\Gamma[x+1]\sim\sqrt{2\pi}x^{x+1/2}e^{-x}$. The *ratio* of the exact to the Stirling approximation is accurate to better than 8.5% for all $1<x<\infty$. This is astonishing, and Stirling's approximation is very useful. Perhaps less well known is that the *difference* between the approximate and exact values is generally huge, reaching about 30 000 for $x=10$, and the *difference* actually diverges as $x\to\infty$. It is the nature of asymptotic approximations that intrinsic limitations exist to their use. Similarly, we believe that asymptotic statements for the consideration of oscillations in amplitudes at current laboratory values would be inappropriate.

B. Perturbatively large *s* versus asymptotically large *s*

Regarding fixed-angle scattering, the factorization scheme and asymptotic limits of the quark-counting model have been tested again and again. We believe that the asymptotic model has been ruled out, and this is progress. All agree that the data [21,22] for $pp\to pp$, $\pi p\to\rho p$, and other spin-dependent processes contradict the ''hadron-helicity conservation'' [23] which is a test of the quark-counting factorization scheme. Meanwhile PQCD with impact-parameter factorization predicts calculable transverse and helicity-violating spin effects for large $s\gg\mathrm{GeV}^2$ [13] due to independent scattering. The large-$s\gg\mathrm{GeV}^2$ perturbative description is self-consistent, and for that reason just as valid as any other application of PQCD.

Quark counting also does not predict the pattern of oscillations cited earlier that are clear evidence for interference effects. Indeed the quark-counting amplitudes are known to have radiative corrections characterized by exponentials of single logarithms, namely real anomalous dimension effects, and cannot produce an energy-dependent phase. However, logarithmic oscillations occur naturally in impact-parameter factorization, and the wavelength of oscillations is calculable [17]. There is sometimes confusion when the two descriptions appear to merge in a further asymptotic approximation, and oscillations disappear [15]. This is a consequence of taking a limit yielding pure power-law dependence, which by analyticity cannot yield an energy-dependent phase.

Finally the literal use of quark-counting factorization cannot encompass color transparency, although color transparency is a closely related phenomenon, indisputably inspired by the ideas of the quark-counting model [1]. The difficulty again is the limit $b \to 0$ assumed in the first step: this limit predicts complete transparency, which is again an asymptotic limit. In order to describe color transparency in PQCD it was necessary to adopt the impact parameter factorization [18]. In a nuclear medium large-b regions interact inelastically with exponential attenuation, while those regions of small b interact proportional to $b^2 \to 0$ [24], resulting in transparency. By depleting the long distance amplitudes, ''nuclear filtering'' enhances the relative contributions of short distance processes in large nuclei [8,9].

One might naively think that the large momentum transfer (Q^2) dependence of color transparency was predicted by quark counting. Unfortunately there is a limit interchange, involving an important scale from the length of the nucleus $R_A \sim A^{1/3}$. The limits of large Q^2 and large A do not commute. Impact parameter factorization predicts that at large $Q^2 \gg \mathrm{GeV}^2$ the survival probability should scale in the variable $Q^2/A^{1/3}$. The BNL data were found to be consistent with this [25]. Attenuation cross sections extracted from the BNL data [26] are also substantially smaller than the traditional 40 mb of conventional strong interaction physics at these energies. Consistently, the cross section in the nuclear target shows negligible oscillations with energy [4] and apparently conforms to predictions of short-distance physics [20,26]. In contrast, a model based on the hadronic basis (Farrar *et al.* [3]) fails to describe the data by many standard deviations. Recent work [27] employing the impact-parameter factorization and PQCD kernels predicts observable color transparency effects in future electron-beam experiments. Preliminary data from CEBAF [28] have been predicted very well [27].

We have, then, a working framework describing numerous interesting and calculable effects unique to the finite s perturbative regime. Unfortunately the calculations at finite s are highly detailed, and there are technical difficulties. A primary difficulty is that there exists no systematic way to extract the most important phase component of a perturbative amplitude. One can readily extract the phase of an amplitude that will dominate the asymptotic limit (the procedure of Ref. [15]), but this is not the same thing as finding a numerically dominant phase coefficient of a numerically dominant amplitude. It is likely that the theory of hadronic physics will have to proceed on a phenomenological basis for some time.

III. CALCULATIONAL TOOLS

In this section we will lay out the components for making calculations. Some of these components are general, some are particular to the experiments at hand, and some have the ambiguities of calculational ''spare parts'' ready for assembly and tuning to make contact with physics.

A. Kinematics and quasiexclusive reactions in nuclei

The kinematics of $2 \to 2$ reactions in free space are familiar and need no review. The situation is more complicated when nuclear and free-space reactions are compared.

Consider a proton in a nucleus with Fermi momentum $k_F \sim 200$–300 MeV. The Fermi momentum is very small compared to the beam momentum $p_{beam} \gg \mathrm{GeV}$. Nevertheless the Fermi momentum can produce a drastic effect on high-energy observables, as follows. Calculate the c.m. energy variable s with its uncertainty Δs due to Fermi momentum by

$$s \pm \Delta s \sim 2[p_{beam}(m \pm k_F)] \sim s_0 \pm 2 p_{beam} k_F .$$

Here s_0 is the nominal c.m. energy variable on a proton at rest. Suppose that the reaction differential cross section goes like a large power of s, for example $\sigma \sim s^{-n}$. Then the effects of Fermi momentum smear reactions over a range of cross sections $\Delta\sigma \sim n\sigma\Delta s/s_0$. It is not hard for the range of variations in cross section to be larger than the cross section. The observable reaction of certain experiments may be dominated by events with the largest cross sections, coming from the configuration where the struck nucleon is moving away from the beam.

These complications were observed in the early stages of the BNL-E850 group, SLAC and CEBAF experiments [4,7]. It is possible to overdetermine the kinematics by measuring several final state momenta: in principle, Fermi momentum can be divided out. The reality includes a good understanding of the acceptance and the errors in the acceptance of the apparatus, which are not our subject. For our purposes, ''quasiexclusive'' reactions in the nuclear target are defined by those reactions satisfying the exclusive criteria, up to corrections of Fermi momenta, and in no case allowing the disruption of color flow caused by emission of a pion. If the experimental observables are adequate, then Fermi motion causes no serious complication: indeed correlations in nuclei can be measured directly and event by event [6]. If the acceptance and resolution do not suffice to determine all the kinematics, then a statistical average over unresolved Fermi momeeta is made. We assume in our calculations that the Fermi momenta has been taken out. Alternatively, our calculations can be smeared as necessary for particular experimental conditions.

B. Phase formulas and the running coupling

The idea of imaginary anomalous dimensions and Sudakov related ''chromo-Coulomb'' phases has been implemented as follows. Inclusion of running coupling effects converts a generic Sudakov exponent from

$$\log^2(Q^2/\Lambda_{IR}) \to \log(Q^2)\log[\log(Q^2/\Lambda^2_{QCD})]. \qquad (1)$$

Here Λ_{IR} and Λ_{QCD} are an infrared cutoff and the QCD running coupling scale, respectively; Q^2 is a large scale controlled by dimensional analysis and the renormalization group (RG). The appearance of Λ_{QCD} suggests a renormalization group origin for the second factor; indeed Λ_{QCD} is defined by its meaning within the RG.

Any amplitude M can be written as $M = \rho e^{i\phi}$. An appropriate renormalization group equation for the phase factor $e^{i\phi}$ must presuppose a *factorization*. The schematic nature of phase factorization is the rule

$$e^{i\phi}(\Lambda_{IR},Q^2;\alpha)=Z(\mu;\Lambda_{IR};\alpha)H(Q^2;\mu;\alpha). \quad (2)$$

Here μ is a renormalization point and $\alpha=g^2/4\pi$ is the coupling constant used diagram by diagram. Leading logarithm approximations suffice to show such factorization for fixed α. We will not show it here, but just assert that factorization applies for $\alpha=\alpha(\mu)$ the running coupling.

Since μ is an arbitrary factorization scale, the total derivative $d/d\mu$ of a physical amplitude is zero, yielding by the chain rule and partial derivative expansion

$$\left[\mu\frac{\partial}{\partial\mu}+\mu\frac{\partial\alpha(\mu)}{\partial\mu}\frac{\partial}{\partial\alpha(\mu)}+i\gamma_\phi[\mu;\alpha(\mu)]\right]\times H(Q^2/\mu^2;\alpha)=0, \quad (3)$$

where

$$i\gamma_\phi[\mu;\alpha(\mu)]=\frac{\mu}{Z}\frac{dZ}{d\mu}$$

is the purely imaginary anomalous dimension appropriate for the phase evolution. Solutions to such equations have been obtained many times [29], and are generally of the form

$$H(\mu,\alpha)=H(\mu_0,\alpha(\mu))e^{i\int_{\mu_0}^{\mu}(d\mu'/\mu')\gamma_\phi[\alpha(\mu')]}.$$

The initial conditions $e^{i\phi(\mu_0)}$ can depend on the infrared cutoff. To lowest order $\gamma_\phi=\gamma_1\alpha$, which can be calculated from a 1-loop diagram. Then given $\alpha_s(\mu)$ and setting $\mu^2\sim Q^2$ as conventional to avoid large logarithms, the phase evolves like

$$e^{i\phi(Q^2)}\sim e^{ic\ \gamma_1\log[\log(Q^2/\Lambda_{QCD}^2)]}. \quad (4)$$

The $i\gamma_\phi$ are color matrices in general, as pointed out in Ref. [16], dealt with by diagonalization before exponentiation, explaining why the constant c is left schematic here.

Dispersion relations relate the real and imaginary parts of amplitudes in field theory. The content of these relations is that amplitudes are analytic, except for singularities near the real axis. A complex function with analytic continuation consistent with Eq. (4) is

$$e^{-S(Q^2;\Lambda_{IR},\Lambda_{QCD})}=e^{-(c\gamma_1/\pi)\log((-Q^2-i\epsilon)/\Lambda_{IR}^2)\log[\log(Q^2/\Lambda_{QCD}^2)]}.$$

This reproduces Eq. (1), and shows that the imaginary anomalous dimensions are invariably associated with Sudakov effects. It also underscores that the phase structure is exceedingly dynamical, depending on the whole s, t, u analytic structure of the particular subprocess. Note that the infrared cutoff contributes to the real but not the imaginary part of the exponent. Reference [15] introduced the transverse impact parameters of quarks to replace infrared cutoffs, and showed how to separate subleading logarithms, at least for the case of the asymptotically leading Landshoff diagrams for $pp\to pp$ studied.

C. Phase phenomenology

Unfortunately, since we no longer have much faith in the asymptotically leading limit, we do not know the amplitudes in much detail. We are obliged to consider a generic series in next to leading logarithms, or powers, all of which are subject to the same pattern of Sudakov corrections and phase evolution. Our rules for ''counting phases on our fingers'' are as follows.

Make a power series ansatz for the amplitude in the large variable Q^2 of the form

$$M_a=(Q^2)^{-B}\sum_{j,k}c_{a;j,k}(Q^2)^{-J}\log(Q^2)^{-k}\times e^{-d_aS(Q^2;\Lambda_{IR},\Lambda_{QCD})}. \quad (5)$$

In other words, respect the quark-counting criteria for the *asymptotically leading* power B, but allow the ansatz to be more general for subasymptotic, perturbatively related subleading powers and logarithms to be incorporated. Compared to the two-component model assumed in Ref. [16], one may include more subleading long distance amplitudes, as illustrated below in Sec. III D.

Continue everything with $Q^2\to -Q^2-i\epsilon$. In doing this, one does not assume that every function crosses a branch cut in some particular process: proper continuations are

$$\log(-s-i\epsilon)\to\log(|s|)-i\pi,$$

$$\log(-t-i\epsilon)\to\log(|t|),$$

$$\log(-u-i\epsilon)\to\log(|u|).$$

The point of continuing everything *as if* timelike is to generate all possibilities.

The result is a ''space'' of trial functions with which to fit free-space data. Examine terms so generated, and select candidates for observable effects, with preference toward terms of most leading order. *A priori* this space is on much the same footing as the quark-counting laws, in the sense that both are consequences of dimensional analysis and general principles. Power law behavior of the data, and logarithmic oscillations with energy, are indications that the ansatz may be relevant.

For nuclear targets, terms with $e^{i\gamma_\phi\log[\log(Q^2/\Lambda_{QCD}^2)]}$ come from naive exponentiation of $\log^2[(-Q^2-i\epsilon)b^2]$, where b is the transverse separation of quarks inside loop integrals. These are long distance amplitudes with Sudakov suppression. Treat these terms in the nuclear case with an eikonalized factor, $I_j=\exp(-\int k\sigma_{jk}ndz)$ where z is the straight-line propagation distance across the target from randomly chosen starting points; n is the nuclear density, and σ_{jk} is a hadron-j-hadron-k absorption cross section of typical strong interaction magnitude. Nuclear filtering is invoked here. Conversely, the short distance amplitudes are attenuated by a model with cross section σ_S which decreases with momentum transfer Q.

Finally, eikonal reactions (''Glauber theory'') of hadrons passing through the nuclear targets can generate constant phases ϕ_A, but not the logarithmically varying kind associated with hard scattering.

This procedure generates predictive power, first by implementing the hypothesis that the free space amplitudes contain mixtures of large and small b regions, explaining the oscillations; second, by attenuating the large b regions with color transparency; and third by predicting the reduction of oscillations in large nuclear targets. In the absence of detailed models, the predictive power of the approach has to be judged objectively: since parameters are used in fitting the data, one takes into account the statistical efffects of the number of parameters compared to other models.

D. Implementation details

We fit the free space data with a two- and a three-component model. The scattering amplitude can be written as

$$M = M_0 + M_1 + M_2,$$

$$\frac{d\sigma}{dt} = \frac{|M_0 + M_1 + M_2|^2}{16\pi s^2}, \tag{6}$$

where M_0 represents a short distance amplitude and M_1, M_2 represent long distance amplitudes. We fit the data including all the three amplitudes M_0, M_1 and M_2 and by keeping only the two amplitudes M_0 and M_1. For the $\pi p \to \pi p$ scattering we parametrize M_0 as

$$M_0 = \frac{\sqrt{16\pi} A_0}{s^3} f(s/t),$$

where $f(s/t)$ is a slowly varying function of s/t and A_0 is a real parameter. The long distance amplitude M_1 is parametrized as

$$M_1 = \frac{\sqrt{16\pi} A_1 \sqrt{s} e^{-ic_1 \log\log Q^2/\Lambda^2_{QCD}}}{s^3 (\log s)^{d_1}} f(s/t),$$

where A_1, c_1 and d_1 are real parameters. M_2 has the same form as M_1 with A_1, c_1 and d_1 replaced by the real parameters A_2, c_2 and d_2 respectively.

The factor Q^2 in the exponent is the momentum transfer squared, namely $Q^2 = -t \approx s/2$ at $\theta_{\text{c.m.}} = 90°$. In accord with the discussion, A_1 and A_2 represent regions of large b, associated Sudakov effects, and logarithmically varying phases, while small-$b \sim 1/Q$ regions should be described by short-distance theory. The $\log s$ factors in the denominator of the A_1, A_2 terms are included to model the additional suppression of large b amplitudes due to the Sudakov form factor. The A_2 term represents a subleading long-distance amplitude compared to the A_1 term.

With these definitions our fit for the differential cross section for the reaction $\pi p \to \pi p$ is given by

$$s^8 \frac{d\sigma}{dt} = \left| A_0 + \frac{A_1 \sqrt{s} e^{-ic_1 \log\log Q^2/\Lambda^2_{QCD}}}{(\log s)^{d_1}} + \frac{A_2 e^{-ic_2 \log\log Q^2/\Lambda^2_{QCD}}}{(\log s)^{d_2}} \right|^2 \tag{7}$$

where s is expressed in units of GeV^2. We have ignored the overall slowly varying function $f(s/t)$ which will not play any role in our analysis.

For the calculation in a nuclear medium we used $\sigma_{pp} = 40$ mb, and $\sigma_{\pi p} = 26$ mb. For the short-distance amplitudes we use a simple model for the attenuation cross section, $\sigma_{S,\pi} = \sigma_{S,p} = k/(x_1 x_2 Q^2)$ with $x_1 = x_2 = 0.5$. The limits of integration on the integral in the exponent of I_j are $-\infty$ to z_0 for the initial state particle and z_0 to ∞ for the final state particle where z_0 is the position of the hard scattering. Short-range nuclear correlations are included [30]. We then calculate the cross section per nucleon in the nuclear case by

$$s^8 \frac{d\sigma_A}{dt} = \frac{N}{A} \int d^3x n(x) \left| A_0 I^i_{S,\pi} I^f_{S,\pi} I^f_{S,p} + \frac{A_1 \sqrt{s} e^{-ic_1 \log\log Q^2/\Lambda^2_{QCD} + i\phi_A}}{(\log s)^{d_1}} I^i_{L,\pi} I^f_{L,\pi} I^f_{L,p} + \frac{A_2 e^{-ic_2 \log\log Q^2/\Lambda^2_{QCD} + i\phi_A}}{(\log s)^{d_2}} I^i_{L,\pi} I^f_{L,\pi} I^f_{L,p} \right|^2 \tag{8}$$

where the superscripts i and f refer to initial and final state attenuation factors, respectively, and A is the nuclear number. N is a normalization factor taking into account the reduction in elastic cross section for configurations which have survived to have a hard collision. In PQCD, this is implemented via integrations over the transverse regions of the hadron wave functions remaining after filtering [27]. The parameter N needs to be fitted from data in the present formalism: we may expect $N \sim 0.3$ on the basis of previous fits. Compared to Ref. [8], which used a similar normalization N_A, the explicit filtering factors account for the A dependence here. Subscripts π and p refer to the particle species suffering attenuation in the nucleus, and S and L refer to short and long distance respectively. The explicit forms of $I^f_{S,\pi}$ and $I^i_{L,\pi}$, for example, are

$$I^f_{S,\pi} = \exp\left(- \int_{z_0}^{\infty} k \sigma_{S,\pi} n dz \right),$$

$$I^i_{L,\pi} = \exp\left(- \int_{\infty}^{z_0} k \sigma_{\pi p} n dz \right).$$

The formula Eq. (8) indicates that we took into account a potential relative phase ϕ_A between the two amplitudes due to interaction with the nucleus: this phase affects the data comparison.

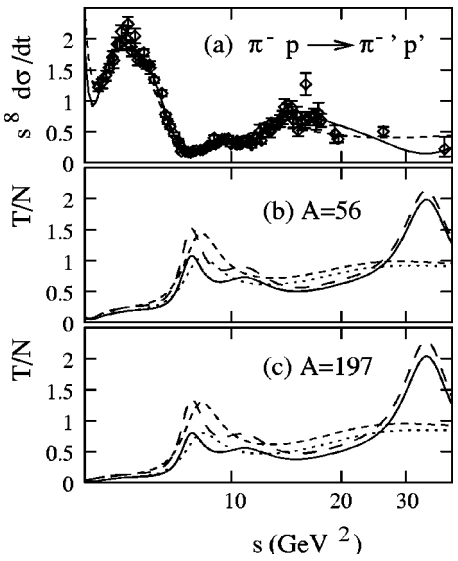

FIG. 1. (a) The free space πp 90° cross section $s^8 d\sigma/dt$ (10^8 GeV^{16} μb/GeV^2) using the model described in Eq. (7) with $A_2 \neq 0$ (solid curve) and with $A_2=0$ (dashed). (b), (c) Calculated color transparency ratio for $A=56,197$ using nuclear filtering, in the model described in Eq. (8) with $A_2 \neq 0$ and $k=10$ (solid), $k=5$ (long dashed) and the model with $A_2=0$ and $k=10$ (dotted) and $k=5$ (short dashed). The y axis is T/N, where T is the transparency ratio and $N<1$ is a normalization parameter to be fitted from data, as discussed in the text. The normalization parameter is defined in Eq. (8).

IV. DATA COMPARISON

Here we compare the basic features of our framework with data and make predictions for reactions with nuclear targets. For now we set the running coupling $\Lambda_{QCD}=200$ MeV; effects of varying this parameter are discussed below.

A. Pion-proton versus pion-nucleus scattering

As our first study, the existence of data for 90° c.m. $\pi^- p \to \pi^- p$ scattering compiled by Blazey [21] [Fig. 1(a)] appears not to be widely appreciated. Oscillations in these data show much the same features as the free-space pp data. Like the corresponding 90° c.m. $pp \to pp$ data, these oscillations of about 50% relative magnitude tend to go unnoticed when plotted on steeply falling logarithmic scales.

The center of mass energy of the data [21] included in our analysis ranges from $s=4.36$ GeV^2 ($Q^2=1.3$ GeV^2) to $s=38.2$ GeV^2 ($Q^2=18.2$ GeV^2). We fit all the data to find the minimum χ^2, defined as the sum of the squares of the difference between data and model, divided by the errors. Explicit calculation shows that χ^2 displays several local minima and hence in order to find the best fit we have to make a careful search in the parameter space. The best fit gives $A_0=-0.638$, $A_1=5.1$, $c_1=25.6$, $d_1=5.13$, $A_2=-0.065$, $c_2=-26.3$, $d_2=-1.16$ with $\chi^2/\mathrm{DOF}=1.97$ (where DOF indicates degrees of freedom). This is not a bad fit: while $\chi^2/\mathrm{DOF}\sim 1$ is the lower limit for testing models, beyond which one has "overfit" a model, $\chi^2/\mathrm{DOF}\sim 2$ is a reasonably good fit with a simple few-component amplitude. All dimensionful parameters are expressed in terms of appropriate powers of GeV. The fit does not change significantly if we delete a few low energy points. If we include only one long distance amplitude setting $A_2=0$, then the best fit gives $A_0=-0.661$, $A_1=-7.67$, $c_1=23.2$, $d_1=6.03$ with $\chi^2/\mathrm{DOF}=5.01$. In comparison the asymptotic model s^{-8} fit gives $\chi^2/\mathrm{DOF}=99$. If we were testing hypothesis here, the asymptotic model would be convincingly ruled out, and radiative corrections from the running coupling and anomalous dimensions evidently could not save it. However the model is somewhat arbitrary, and its predictive power is not in the goodness of fit, but in the next step of application to nuclear targets.

We turn to the corresponding pion-initiated reaction with a nuclear target. We treat ϕ_A and k as parameters subject to considerable uncertainty. However for the entire range of $0<\phi_A<2\pi$ and varying $5<k<10$ the calculations are sufficiently robust to predict rather dramatic effects. In Fig. 1(b) we show the results for the transparency ratio,

$$T(Q^2,A)=\frac{d\sigma(\pi A\to m'N'(A-1);90°)/dt}{[Zd\sigma(\pi p\to\pi' p';90°)/dt]} \qquad (9)$$

for the two different models. The plots [Figs. 1(b), 1(c)] show a striking 180° phase shift between the oscillations of the transparency ratio and those seen in the free-space reaction. $T(Q^2,A)$ is less sensitive to variations of ϕ_A compared to k: for all values of the ϕ_A we find that $T(Q^2,A)$ shows significant oscillations with energy. Only for very large values of $k \gg 10$ do these oscillations disappear, a limit in which no short distance contribution effectively exists. In this limit the transparency ratio is very sensitive to the nuclear phase ϕ_A since even in the nuclear medium all the interfering amplitudes have roughly equal strength. The plots (Fig. 1) are given for large nuclei where the calculation indicates filtering will be effective: for $A \gg 1$, the impact parameter factorization predicts [25] scaling in the variable $Q^2/A^{1/3}$. The theory may be extended to smaller $A \approx 12$, where our calculations also show a substantial effect, with less confidence regarding the importance of the short-distance component.

As in the pp case, the measurement of the transparency ratio as a function of s should show behavior contradicting conventional strong interaction physics. Observation of this would be extremely interesting. The A dependence at fixed large s is also pivotal: the effective cross sections that can be extracted should be capable of ruling out the hadronic-basis predictions for the same reaction, which are either monotonic in energy (Glauber theory) or linear in the energy [pointlike classical expansion theory (Farrar *et al.* [3])].

Multiple minima and running coupling effects

We next discuss the effect of varing the QCD scale parameter Λ_{QCD} on our predictions for the transparency ratio. We varied Λ_{QCD} from 100 MeV to 300 MeV. The resulting free space parameters for the fit obtained by varing Λ_{QCD} are given in Tables I and II for the two and three component fits respectively. In Table II we have also included the param-

TABLE I. The parameter values for the different fits to the $\pi p \to \pi p$ cross section corresponding to the two amplitude model. The fits 1, 2, and 3 correspond to the QCD scale parameter $\Lambda_{QCD} = 0.1$, 0.2, and 0.3 GeV respectively. All the parameters are given in units of an appropriate power of GeV, as explained in text.

Fit no.	Λ_{QCD}	A_0	A_1	c_1	d_1	χ^2/DOF
1	0.1	−0.655	8.79	32.1	6.25	5.03
2	0.2	−0.661	−7.67	23.2	6.03	5.01
3	0.3	−0.654	10.3	19.6	6.51	4.77

eters corresponding to a local minimum in χ^2 which gives a χ^2 slightly larger than that obtained in the case of absolute minima. These fits are also interesting despite the fact that it is not the absolute minimum in χ^2. In the two component case we give results only for the global minima since the remaining fits give very large χ^2. The statistical interpretation of χ^2 is meaningful at any local minimum, and does not exclude the existence of multiple minima. The resulting fits for the three component model are shown in Fig. 2. We find that the fits do not change too much as a function of Λ_{QCD}. The fits 3 and 5 which correspond to a local minimum do, however, show significant deviation from the fits 1, 2, and 4 in the region where the available data are rather scarce. Our predictions for the transparency ratio for the two and three component models are shown in Figs. 3 and 4 respectively. The parameter k has been set equal to 7 for this calculation. We find for the two component model that the transparency ratio does not show a large deviation as a function of Λ_{QCD}. In the case of the three component model, however, the deviation as a function of Λ_{QCD} is larger in the region where free space data are scarce.

For the case of local minima, corresponding to fits 3 and 5, the transparency ratio shows a completely different behavior. It is much smaller than that obtained for the case of an absolute minimum. The oscillations are still obtained, however, and are observable 180° out of phase with the oscillations seen in free space. At large values of s the oscillations in T are shifted compared to those seen in the case of absolute minima. This happens because at large s the free space data are scarce and these two fits differ considerably in this

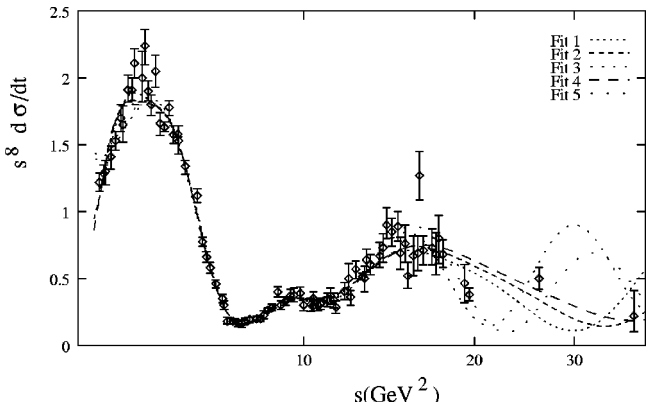

FIG. 2. Comparison of different fits to free space $\pi p \to \pi' p'$ scattering data using the three component model. The parameter values of the fit are given in Table II. The fit 1 uses $\Lambda_{QCD} = 0.1$ GeV, fits 2 and 3 use $\Lambda_{QCD} = 0.2$ GeV and fits 4 and 5 use $\Lambda_{QCD} = 0.3$ GeV.

region as can be seen from Fig. 2. The reason for the large difference in the transparency ratio for the case of fits 3 and 5 in comparison to fits 1, 2, and 4 can be understood as follows. The absolute value of the parameter A_0 for fit 3, for example, is less than half its value for fit 2. In the nuclear medium the long distance terms are filtered out which means that the contribution of the A_1 and A_2 terms is negligible. Hence the normalization of the transparency ratio for fit 3 is expected to be one fourth of what is obtained for fit 2. This explains the large reduction in the normalization of the transparency ratio in the cases of fits 3 and 5. We point out that in the cases of fits 3 and 5, the relative contributions of the long distance terms are larger in free space in comparison to fits 1, 2 and 4. Although the normalizations A_1 and A_2 of these terms are also reduced in proportion to A_0 we also need to take into account the logarithmic denominators. In the region of interest these factors give a relative enhancement of the fits 3, for example, compared to fit 2. Hence the long distance terms in fits 3 and 5 are larger in free space compared to fits 1, 2, and 4. It is interesting that such fits give further justification of the overall normalization parameter introduced in Ref. [8] to fit the experimental result for the transparency ratio.

TABLE II. The parameter values for the different fits to the $\pi p \to \pi p$ cross section corresponding to the three amplitude model. We give results for three different choices of the QCD scale parameter Λ_{QCD}. All the parameters are given in units of an appropriate power of GeV, as explained in text. For each of the chosen values of Λ_{QCD} we give two different types of fit which correspond to two different minima in χ^2, such that the χ^2 for these two fits is very close. For the case of $\Lambda_{QCD} = 0.1$ we give results for only one fit since the second fit was found at a very large value of χ^2.

Fit no.	Λ_{QCD}	A_0	A_1	c_1	d_1	A_2	c_2	d_2	χ^2/DOF
1	0.1	−0.623	6.49	36.0	5.51	−0.044	−36.5	−1.61	1.81
2	0.2	−0.638	5.1	25.6	5.13	−0.065	−26.3	−1.16	1.97
3	0.2	−0.305	2.19	25.6	2.99	−0.0039	−22.5	−4.28	2.12
4	0.3	−0.651	4.43	19.9	4.92	−0.087	−20.7	−0.76	2.26
5	0.3	−0.308	2.05	19.8	2.88	0.0046	−18.7	−4.01	2.06

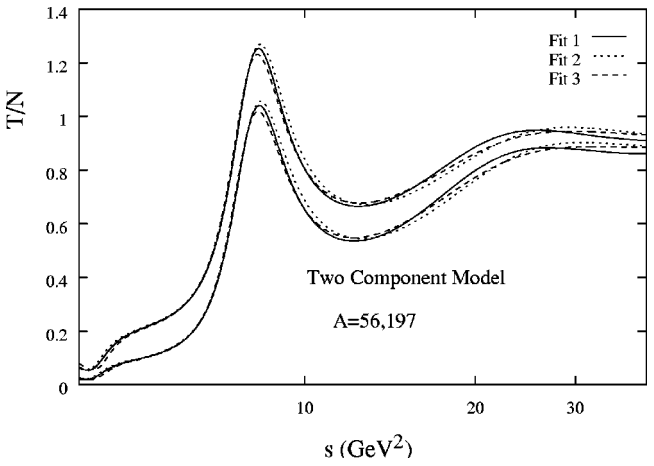

FIG. 3. The dependence of the predicted color transparency ratio on the QCD scale parameter Λ_{QCD} for the two component model. The upper three curves are for nuclear number $A=56$ and the lower three curves use $A=197$. The parameter values corresponding to the different fits to the free space $\pi p \to \pi' p'$ scattering data are given in Table I. The fits 1, 2 and 3 use $\Lambda_{QCD}=0.1$, 0.2 and 0.3 GeV respectively. T/N is defined in Fig. 1.

B. Photon-proton versus photon-nucleus scattering

Most exciting are experimental data and rapidly upcoming prospects for the processes $\gamma p \to \pi^+ n$ and $\gamma n \to \pi^- p$. Data exist for $s<16$ GeV^2 and $s<4$ GeV^2, respectively [31]. The Jefferson Lab and CEBAF are soon expected to extend the energy range of γn reactions to about $s=16$ GeV^2 with high precision, as well as measure the color transparency ratio for this process [10].

The short distance theory predicts $d\sigma/dt_{90°} \sim s^{-7}$, within which framework it has been shown for asymptotically large momentum transfer [32] that Landshoff pinches are absent. Unlike pp and πp reactions, then, where the pinch regions actually constitute the asymptotic prediction, here the Landshoff and associated Sudakov phase physics is subleading. But the asymptotic limit (infinite energy) has little weight for laboratory energy, and there are pinches at subleading order, which we will investigate.

Most interestingly, the existing data show considerable oscillations around power dependence [Fig. 5(a)]. Like the π-p case, the existence of these data also appears not to be widely appreciated. We fit the experimental data for $\gamma p \to \pi^+ n$ with center of mass scattering angle 90° and $\sqrt{s}>2$ GeV. The center of mass energy of the data ranges from $\sqrt{s}=2.38$ GeV ($Q^2=1.96$ GeV^2) to $\sqrt{s}=3.867$ GeV ($Q^2=6.6$ GeV^2). The cut $\sqrt{s}>2$ GeV is imposed so as to select high energy data where the perturbative treatment is most likely to be applicable.

We use the same amplitude ansatz as Eq. (7) for $s^7 d\sigma/dt$, but with the A_1 and A_2 terms containing an additional factor of s in the denominator. We do this because the Landshoff pinches are absent at leading power. We obtain $A_0=0.90$, $A_1=2.65/s$, $c_1=64.5$, $A_2=8.01/s$, $c_2=-126.4$ with $\chi^2/\mathrm{DOF}=0.69$. All dimensionful parameters are expressed in units of appropriate powers of GeV. We have set $d_1=d_2=4$, as the quality of fit does not depend substantially on these parameters. The values of d_1 and d_2 were chosen to obtain a relatively flat free-space behavior beyond $\sqrt{s}=3.0$ GeV, where the presence or absence of oscillations remains experimentally unstudied. We arbitrarily imposed a model of short-distance physics for this region.

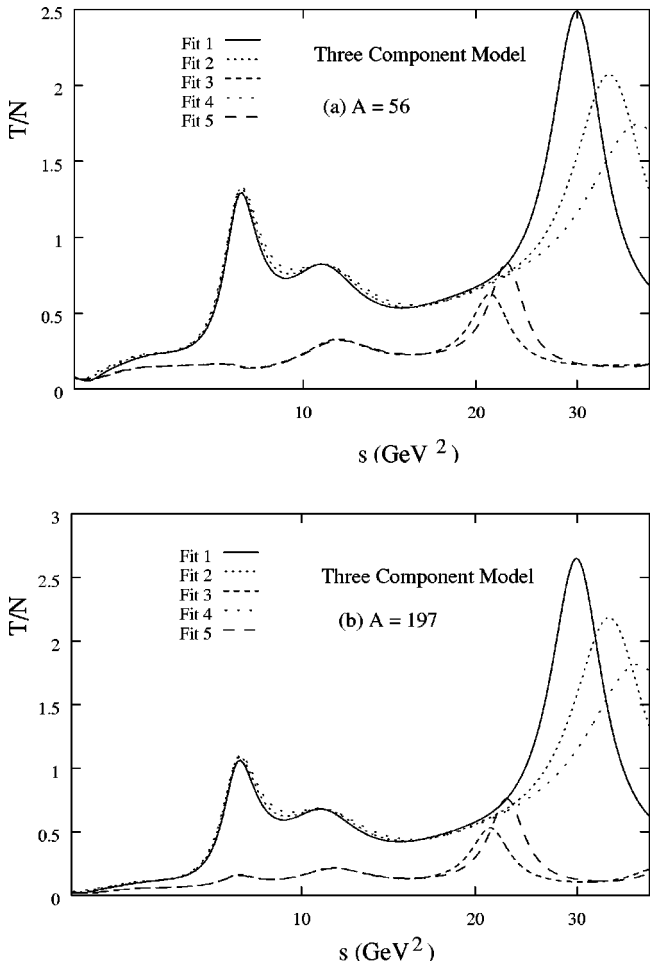

FIG. 4. Comparison of the predicted color transparency ratio corresponding to the three component model for (a) $A=56$ and (b) $A=197$. The parameter values corresponding to the different fits to the free space $\pi p \to \pi' p'$ scattering data are given in Table II. The fit 1 uses $\Lambda_{QCD}=0.1$ GeV, fits 2 and 3 use $\Lambda_{QCD}=0.2$ GeV and fits 4 and 5 use $\Lambda_{QCD}=0.3$ GeV. T/N is defined in Fig. 1.

The best fit to the 17 data points available is shown in Fig. 5. As in the case of πp scattering, the fit does not change significantly if a few low energy data points are deleted. If we set $A_2=0$ then the best fit gives $A_0=0.89$, $A_1=-4.15$ and $c_1=79.8$ with χ^2 per degree of freedom of 1.09. For comparison the short-distance s^{-7} model gives $\chi^2/\mathrm{DOF}=2.9$. While our fit is favored statistically, including effects of extra parameters, the short-distance model is not ruled out in this comparison. Cutting the experimental uncertainties in half would be decisive. We mention this because the uncertainties are expected to decrease with the imminent experiments.

For the nuclear process $\gamma A \to \pi^+ n(A-1)$, we calculate $s^7 d\sigma/dt$ with the same format as Eq. (8). Results for the transparency ratio for $A=12,56,197$ are shown in Fig. 5. In

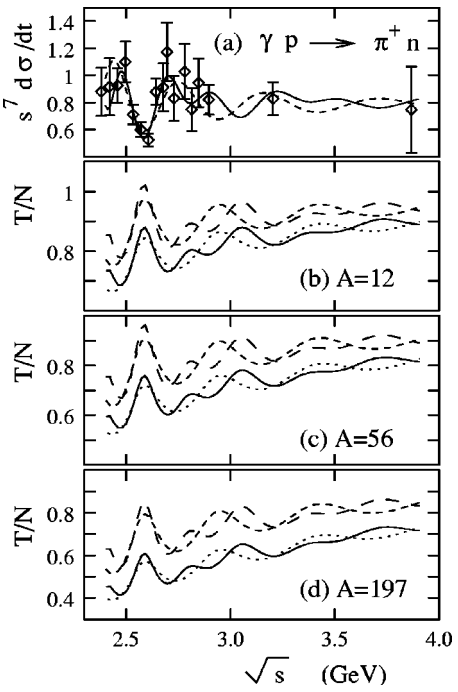

FIG. 5. (a) The free space $\gamma p \to \pi^+ n$ 90° cross section $s^7 d\sigma/dt(10^7\ \mathrm{GeV}^{14}\,\mathrm{nb/GeV}^2)$ using the model described in Eq. (7) with $A_2 \neq 0$ (solid curve) and with $A_2 = 0$ (dashed). (b),(c),(d) Calculated color transparency ratio for $A = 12,56,197$ using nuclear filtering, in model described in Eq. (8) with $A_2 \neq 0$ and $k = 10$ (solid), $k = 5$ (long dashed), and the model with $A_2 = 0$ and $k = 10$ (dotted) and $k = 5$ (short dashed). T/N is defined in Fig. 1.

calculating filtering factors we conservatively assume that the incident photon does not attenuate significantly. While there are many models to attenuate the photon somewhat, this choice allows a conservative presentation. Otherwise the effects of filtering, which generate the oscillating transparency ratio, would be larger, creating more dramatic oscillations. Of course some information can be gathered on the incoming photon cross section by studying the magnitude of oscillations when they are observed. Let us note that experimentally the final state N can be a proton or a neutron, but to predict the neutron case definitively we would need free space neutron scattering data that we do not currently have.

TABLE III. The parameter values for the different fits to the $\gamma p \to \pi^+ n$ cross section corresponding to the two amplitude model. The fits 1, 2 and 3 correspond to the QCD scale parameter Λ_{QCD} = 0.1, 0.2 and 0.3 GeV respectively. All the parameters are given in units of an appropriate power of GeV, as explained in text.

Fit no.	Λ_{QCD}	A_0	sA_1	c_1	χ^2/DOF
1a	0.1	0.887	4.17	108.6	1.09
1b	0.1	0.884	−3.96	95.7	1.17
2a	0.2	0.887	−4.15	79.8	1.09
2b	0.2	0.885	−3.96	70.9	1.18
3a	0.3	0.887	4.17	65.6	1.09
3b	0.3	0.885	−3.99	57.7	1.16

TABLE IV. The parameter values for the different fits to the $\gamma p \to \pi^+ p$ cross section corresponding to the three amplitude model. We give results for three different choices of the QCD scale parameter Λ_{QCD}. All the parameters are given in units of an appropriate power of GeV, as explained in text. For each of the chosen values of Λ_{QCD} we give two different types of fit which correspond to two different minima in χ^2, such that the χ^2 for these two fits is very close.

Fit no.	Λ_{QCD}	A_0	sA_1	c_1	sA_2	c_2	χ^2/DOF
1a	0.1	0.902	2.74	83.1	8.27	−163.8	0.69
1b	0.1	0.860	−15.1	55.2	−29.8	−75.2	0.82
2a	0.2	0.90	2.65	64.5	8.01	−126.4	0.69
2b	0.2	0.851	−13.3	44.4	26.4	−52.9	0.87
3a	0.3	0.904	2.73	50.2	8.46	−97.0	0.68
3b	0.3	0.853	14.5	34.1	−28.8	−44.3	0.78

Observing Fig. 5, the predicted transparency ratio $T(Q^2,A)$ again oscillates 180° out of phase with the free space cross section. The overall normalization parameter in the nuclear medium has been set equal to unity and can be adjusted to fit the normalization of the experimental data once they are available. The nuclear phase has also been ignored in the calculation of the transparency ratio. Previous hadronic-basis estimates for the transparency ratio have not taken the oscillations in free space data into account, yielding monotonically increasing energy dependence [10]. The upcoming photon-initiated experiments, then, may be on the verge of confirming a third case of oscillating fixed angle data, and oscillating color transparency.

Color transparency with a photon beam remains significantly different from hadron initiated processes. The distinction becomes clear when the Q^2 dependence of a virtual photon is used as an experimental tool. In the limit of large $Q^2 \gg \mathrm{GeV}^2$, experimental evidence from deeply inelastic scattering provides overwhelming support to the concept of a pointlike photon interaction, with negligible attenuation and perturbatively understood hadronic components in scattering.

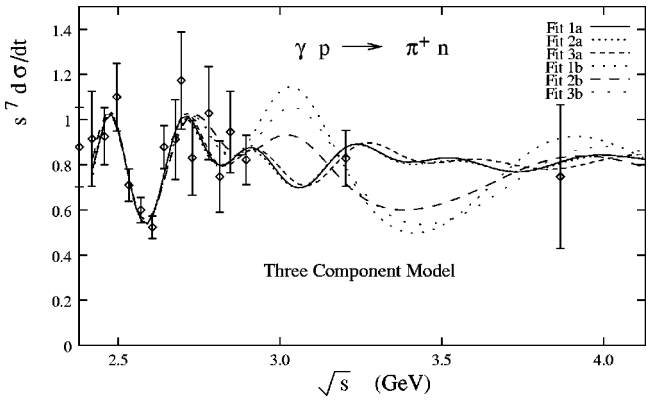

FIG. 6. Comparison of different fits to free space $\gamma p \to \pi^+ n$ scattering data using the three component model. The parameter values of the fit are given in Table IV. The fits 1a and 1b use $\Lambda_{QCD} = 0.1$ GeV, fits 2a and 2b use $\Lambda_{QCD} = 0.2$ GeV and fits 3a and 3b use $\Lambda_{QCD} = 0.3$ GeV.

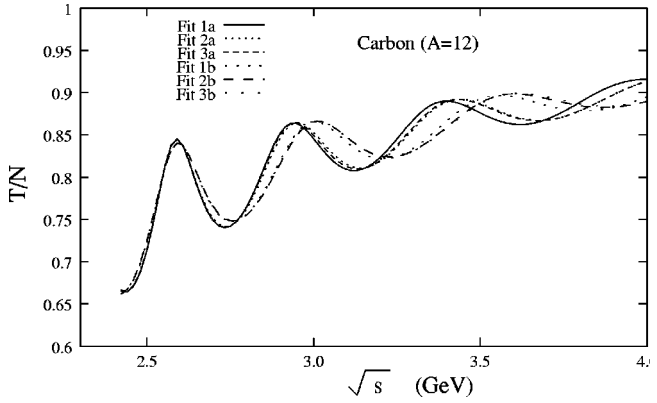

FIG. 7. Predictions for color transparency for $\gamma p \to \pi^+ n$ for different two component models. The parameters corresponding to the free space fit are given in Table III. T/N is defined in Fig. 1.

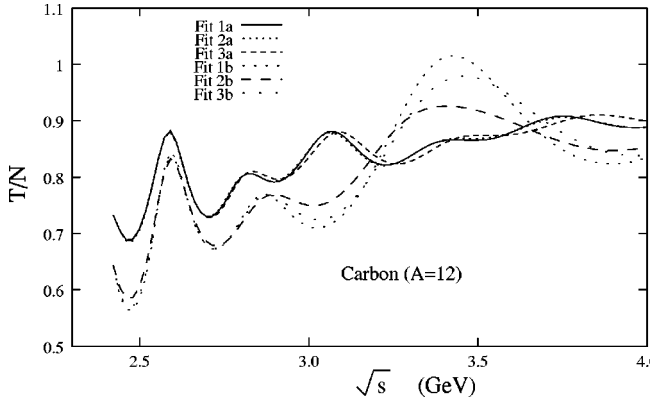

FIG. 8. Predictions for color transparency for $\gamma p \to \pi^+ n$ for different three component models. The parameters corresponding to the free space fit are given in Table IV. T/N is defined in Fig. 1.

The lack of pinch singularities of the short distance framework predicts fading of oscillations by an inverse power law at large Q^2. Fading of oscillations should occur in both the free space cross section and the transparency ratio in the limit of $Q^2 \gg \mathrm{GeV}^2$. The regime of large Q^2 for photons should coincide with the regime of Bjorken scaling, so that the moderate Q^2 of existing electron beams should suffice. This would be an extremely interesting and productive area to explore experimentally.

We again investigate the Λ_{QCD} dependence of our predicted transparency ratio. The fits for different values of Λ_{QCD} are given in Tables III and IV for the two and three component models respectively. We have also given results for a local minimum which gives the next larger value of χ^2 above the absolute minimum for all the cases. The resulting fits to the free space data are displayed in Fig. 6. Our predictions for the transparency ratio corresponding to the two and three component models are shown in Figs. 7 and 8 respectively. The parameter k has been set equal to 10 for this calculation. We again find that the predicted transparency ratio varies only by a small amount as the Λ_{QCD} is varied from 100 to 300 MeV. However the predictions for the local minima do show significant differences from the results obtained with the absolute minimum especially in the region where the available free space data are very scarce.

C. Hadron-helicity conservation or nonconservation

Direct tests of the hadron-helicity nonconserving character of the pinch-singularity regions are very interesting. Perturbative QCD explains these effects [13] as consequences of quark orbital angular momentum, generating certain interesting predictions.

A pion beam suggests studying reactions involving a final-state ρ meson: again the process has pinch singularities. The PQCD analysis indicates that oscillations of fixed-angle scattering with energy will occur, and indeed one of the points of this paper is that such oscillations are *generic*. The failure of short-distance models, and dynamical importance of the pinch regions for $\pi p \to \rho p$ is supported by observations [22] of final-state ρ-polarization density matrix elements $\rho_{1,-1}$ of order unity. If this is due to the pinch regions, as currently expected [12,13], then filtering in a large nucleus should remove them. Oscillating polarization effects would be very dramatic: $\rho_{1,-1}$ oscillating with energy at fixed angle is expected if the dynamical phases are correlated with exchange of orbital angular momentum. Counting powers of the internal coordinate b and the units of orbital angular momentum, we can predict that at fixed large Q^2, each power of b^2 in amplitude calculations will scale as $A^{-1/3}$ due to nuclear filtering. This counting is a short-distance estimate, and so represents a maximal effect: it an experimental question whether it would be achieved, but in no event would we predict stronger suppression.

V. CONCLUDING REMARKS

Oscillating color transparency is a generic prediction of PQCD, testable with imminent experiments. We believe that the observation of oscillations in experimental data for the transparency ratio, consistently 180° out of phase with the free space counterparts, and in three independent reactions, will be strong confirmation of nuclear filtering and the basic PQCD understanding of color transparency.

ACKNOWLEDGMENTS

We thank Haiyan Gao and Dipangkar Dutta for very useful discussions and for providing data for γp. We also thank Gerry Blazey for help with data and Bernard Pire for helpful comments. This work was supported in part under the Department of Energy Grant Number DE-FG02-98ER41079, and the Kansas Institute for Theoretical and Computational Science/ K*STAR program.

[1] S.J. Brodsky and A.H. Mueller, Phys. Lett. B **206**, 685 (1988); S.J. Brodsky, in *Proceedings of the 13th International Symposium on Multiparticle Dynamics*, Vollendam, 1982, edited by W. Kittel *et al.* (World Scientific, Singapore, 1982); A.H. Mueller, in *Proceedings, Rencontres de Moriond Les Arcs, France, 1982*, edited by J. Tran Thanh Van (Editions Frontieres, Gif-sur-Yvette, 1982).
[2] P. Jain, B. Pire, and J.P. Ralston, Phys. Rep. **271**, 67 (1996).
[3] G.R. Farrar, H. Liu, L.L Frankfurt, and M.I. Strikman, Phys. Rev. Lett. **64**, 2996 (1990); B.K. Jennings, and G.A. Miller, Phys. Lett. B **318**, 7 (1993); O. Benhar, S. Fantoni, N.N. Nikolaev, J. Speth, A.A. Usmani, and B.G. Zakharov, Z. Phys. A **355**, 191 (1996); S. Frankel, and W. Frati, Phys. Lett. B **291**, 368 (1992); A. Kohama, K. Yazaki, and R. Seki, Nucl. Phys. **A536**, 716 (1992).
[4] A.S. Carroll *et al.*, Phys. Rev. Lett. **61**, 1698 (1988); S. Heppelmann, Nucl. Phys. B (Proc. Suppl.) **12**, 159 (1990).
[5] E850 Collaboration, A. Leksanov *et al.*, Phys. Rev. Lett. **87**, 212301 (2001); see also in *Intersections of Particle and Nuclear Physics*, edited by Zohreh Parsa and William J. Marciano, AIP Conf. Proc. No. 549 (AIP, Melville, NY, 2000), nucl-ex/0009008.
[6] J. Aclander *et al.*, Phys. Lett. B **453**, 211 (1999).
[7] N. Makins *et al.*, Phys. Rev. Lett. **72**, 1986 (1994); T.G. O'Neill *et al.*, Phys. Lett. B **351**, 87 (1995).
[8] J.P. Ralston and B. Pire, Phys. Rev. Lett. **61**, 1823 (1988).
[9] S.J. Brodsky and G.F. de Teramond, Phys. Rev. Lett. **60**, 1924 (1988).
[10] H. Gao and R.J. Holt, Jefferson Lab experiment E94-104.
[11] S.J. Brodsky and G.P. Lepage, Phys. Rev. D **24**, 2848 (1981).
[12] P.V. Landshoff, Phys. Rev. D **10**, 1024 (1974).
[13] T. Gousset, B. Pire, and J.P. Ralston, Phys. Rev. D **53**, 1202 (1996).
[14] J.C. Polkinghorne, Phys. Lett. **49B**, 277 (1974).
[15] J. Botts and G. Sterman, Phys. Lett. B **224**, 201 (1989); Nucl. Phys. **B325**, 62 (1989).
[16] B. Pire and J.P. Ralston, Phys. Lett. **117B**, 233 (1982); J.P. Ralston and B. Pire, Phys. Rev. Lett. **49**, 1605 (1982).
[17] A. Sen, Phys. Rev. D **28**, 860 (1983).
[18] J.P. Ralston and B. Pire, Phys. Rev. Lett. **65**, 2343 (1990).
[19] A.H. Mueller, Phys. Rep. **73**, 237 (1981).
[20] V.A. Matveev, R.M. Muradyan, and V.A. Tavkhelidze, Lett. Nuovo Cimento Soc. Ital. Fis. **7**, 719 (1973); S.J. Brodsky and G.R. Farrar, Phys. Rev. D **11**, 1309 (1975).
[21] D.P. Owen *et al.*, Phys. Rev. **181**, 1794 (1969); K.A. Jenkins *et al.*, Phys. Rev. D **21**, 2445 (1980); C. Baglin *et al.*, Nucl. Phys. **B216**, 1 (1983); J. Blazey, Ph.D. thesis, University of Minnesota, 1986.
[22] S. Heppelmann *et al.*, Phys. Rev. Lett. **55**, 1824 (1985).
[23] C. Carlson, V. Chashkuhnashvilli, and F. Myhrer, Phys. Rev. D **46**, 2891 (1992); P. Ramsey and D. Sivers, *ibid.* **52**, 116 (1995).
[24] F. Low, Phys. Rev. D **12**, 163 (1975); S. Nussinov, Phys. Rev. Lett. **34**, 1286 (1975); F. Gunion and D.E. Soper, Phys. Rev. D **15**, 2617 (1977); G. Bertsch, S.J. Brodsky, A.S. Goldhaber, and J.C. Gunion, Phys. Rev. Lett. **47**, 297 (1981).
[25] P. Jain and J.P. Ralston, in *Proceedings of the XXVIII International Rencontre de Moriond: QCD and High Energy Hadronic Interactions*, Les Arcs, France, 1993, edited by J. Tranh Van Thanh (Editions Frontieres, Gif-Sur-Yvette, 1994); in *International Conference on Elastic and Diffractive Scattering*, Brown University, Providence, Rhode Island, 1993 (World Scientific, Singapore, 1994); in *PAN XIII: The International Conference on Particles and Nuclei in Collision*, Perugia, Italy, 1993, edited by A. Pascolini (World Scientific, Singapore, 1994); B. Pire and J.P. Ralston, Phys. Lett. B **256**, 523 (1991).
[26] P. Jain and J.P. Ralston, Phys. Rev. D **48**, 1104 (1993).
[27] B. Kundu, J. Samuelsson, P. Jain, and J.P. Ralston, Phys. Rev. D **62**, 113009 (2000); P. Jain, B. Kundu, J.P. Ralston, and J. Samuelsson, Fiz. B **8**, 345 (1999); B. Kundu, H.-N. Li, J. Samuelsson, and P. Jain, Eur. Phys. J. C **4**, 637 (1999).
[28] K. Garrow (private communication).
[29] See, e.g., Stefan Pokorski, *Gauge Field Theories* (Cambridge University Press, Cambridge, England, 1987), Chap. 6.
[30] G.A. Miller and J.E. Spencer, Ann. Phys. (N.Y.) **100**, 562 (1976); T.S.H. Lee and G.A. Miller, Phys. Rev. C **45**, 1863 (1992).
[31] R.L. Anderson *et al.*, Phys. Rev. D **14**, 679 (1976).
[32] G. Farrar, G. Sterman, and H. Zhang, Phys. Rev. Lett. **62**, 2229 (1989).